Spin, Charge, and Orbital Ordering in $La_{0.5}Sr_{1.5}MnO_4$

Priya Mahadevan,[1,*] K. Terakura,[2,] and D. D. Sarma[3,†]

[1]*JRCAT and AIST, Tsukuba, Ibaraki 305-0046, Japan*
[2]*JRCAT, Tsukuba, Ibaraki 305-8562, Japan*
and RICS-AIST, Tsukuba, Ibaraki 305-8568, Japan
[3]*SSCU, Indian Institute of Science, Bangalore 560012, India*

We have analyzed the experimental evidence of charge and orbital ordering in $La_{0.5}Sr_{1.5}MnO_4$ using first principles band structure calculations. Our results suggest the presence of two types of Mn sites in the system. One of the Mn sites behaves as an Mn^{3+} ion, favoring a Jahn-Teller distortion of the surrounding oxygen atoms, while the distortion around the other is not a simple breathing mode kind. Band structure effects are found to dominate the experimental spectrum for orbital *and charge ordering,* providing an alternate explanation for the experimentally observed results.

PACS numbers: 71.20.–b, 61.10.Dp

In recent times there has been a resurgence of interest in the manganites as a result of the wide range of physical properties that they exhibit. In some of the doped compounds, there is a real space ordering of the charge carriers in certain orbitals, resulting in orbital ordering (OO) and sometimes charge ordering (CO). As the magnetic and transport properties are closely correlated with the orbital and charge degrees of freedom, there have been intense efforts—both experimental and theoretical—to clarify the microscopic mechanisms giving rise to such exotic phenomena [1]. While techniques such as electron microscopy and neutron scattering have been traditionally used to detect CO as well as magnetic ordering [2], the direct observation of OO has been difficult. Murakami *et al.* performed pioneering experiments on $LaMnO_3$ [3] and $La_{0.5}Sr_{1.5}MnO_4$ [4] and were successfully able to detect OO. The technique they used exploited the anisotropy of the x-ray scattering tensor at an absorption edge, thereby making the intensity of the scattered x rays sensitive to the valence electron distribution.

$La_{0.5}Sr_{1.5}MnO_4$ is a layered manganite with an average valence of 3.5 at each Mn site. In the high temperature phase, above the CO temperature, all Mn-O bond lengths within the *ab* plane are equal [5]. Neutron scattering studies by Sternlieb *et al.* [6] indicated a real space ordering of two distinct Mn sites below 217 K, with the two sites identified as Mn^{3+} and Mn^{4+}. The intensity variation observed at the two sites was interpreted as arising from a 1% breathing modelike movement of the oxygen atoms in the *ab* plane towards one set of Mn atoms, identified as the higher valent Mn^{4+} sites. Later experiments by Murakami *et al.* [4] used the anisotropy of the x-ray scattering tensor to show that the Mn sites form a pattern of alternating Mn^{3+}-Mn^{4+} sites in the *ab* plane, with both CO and OO taking place at the same temperature, 217 K. They claimed that the charge modulation between the two Mn sites is not small, but corresponds to as much as an *integral* charge fluctuation between neighboring Mn sites. However, if this is the case, strong correlations are necessary

to localize charge carriers. Surprisingly, however, certain other spectroscopic properties [7] of this system can be easily explained by a single particle approach.

The contrasting experimental evidence, where one set of spectroscopic data could be easily explained by an effective single particle approach, while another set implied the importance of strong correlations in the system, prompted us to perform a detailed analysis of the electronic structure using the density-functional pseudopotential framework. Apart from providing a microscopic mechanism for the observed *orbital and charge ordering* in this system, our results have important implications on recent anomalous x-ray scattering experiments on $Pr_{1-x}Ca_xMnO_3$ [8], $LaSr_2Mn_2O_7$ [9], and NaV_2O_5 [10].

The details of the computational method are described elsewhere [11], and we mention only minimum additional aspects. The cutoff energy for the plane wave expansion of the eigenstate is 20 Ry, being smaller than the value of 30.25 Ry in our usual calculations because of the large unit cell in the present calculation. The *k*-point mesh used is $4 \times 4 \times 2$. The generalized gradient approximation was used for the exchange functional [12]. The alloying effects of $(La_{0.5}Sr_{1.5})$ at the *A* site of the lattice are treated within the virtual crystal approximation [13].

The Mn spins order below 110 K forming one-dimensional ferromagnetic zigzag chains in the *ab* plane coupled antiferromagnetically to each other, known as the CE-type magnetic ordering. As the exchange splitting is large (about 3 eV), the amplitude for electrons to hop from a zigzag chain of parallel spins (indicated by thick solid lines in Fig. 1a) to the neighboring chain is small. Hence the electronic structure is governed by these one-dimensional chains. Considering a single chain, it was shown [14] that the anisotropic hopping between the Mn *d* orbitals could explain the OO at the two Mn sites. We have performed *ab initio* calculations considering the complete three-dimensional *Immm* structure [5]. Similar to the findings in Ref. [14], we also found the kind of OO that is observed experimentally. Choosing the *x*
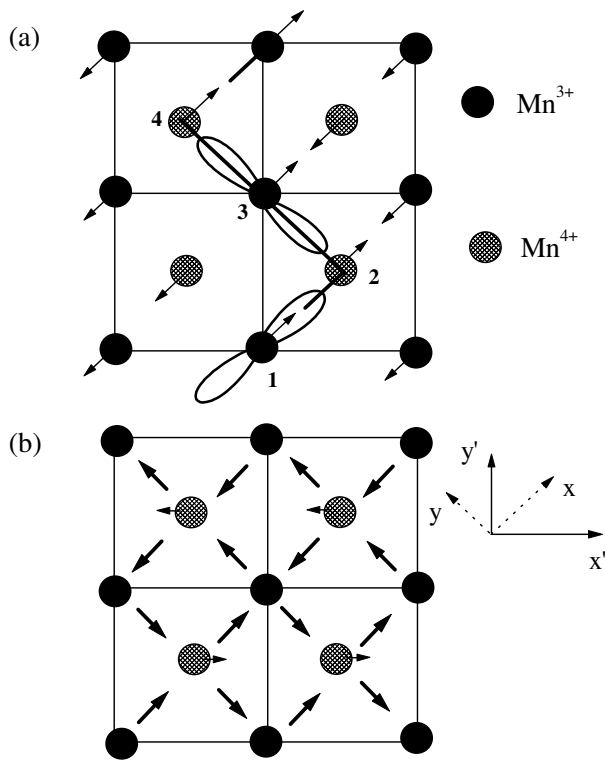
FIG. 1. (a) A schematic diagram of the spin, charge, and orbital ordering of the Mn atoms in the ab plane. The magnetic structure consists of the zigzag chain (thick solid line connecting atoms 1, 2, 3, and 4), coupled antiferromagnetically to the neighboring chains. (b) The directions of displacements of the oxygen atoms when the atom positions are relaxed are shown by the thick arrows, while the displacements of the Mn^{4+} atoms (~ 0.015 Å) are indicated by the small arrows. The two choices of coordinate axes x and y and x' and y' used are shown.

and y axes as shown in Fig. 1, we found that while the $d_{3x^2-r^2}$ orbital was preferentially occupied on atom 1, the $d_{3y^2-r^2}$ orbital was preferentially occupied on atom 3. These results can be understood within the framework of a simple nearest neighbor tight-binding model involving the e_g orbitals: $d_{3x^2-r^2}$ and $d_{y^2-z^2}$ on atom 1, $d_{3y^2-r^2}$ and $d_{z^2-x^2}$ on atom 3, as well as $d_{3z^2-r^2}$ and $d_{x^2-y^2}$ on atoms 2 and 4 as used in Ref. [14]. While the $d_{3x^2-r^2}$ orbital at Mn(1) and $d_{3y^2-r^2}$ orbital on Mn(3) hybridize with both e_g orbitals on atoms 2 and 4, the $d_{y^2-z^2}$ on Mn(1) and $d_{z^2-x^2}$ on Mn(3) do not. The eigenvalue spectrum of such a simple model consists of two bonding bands, energetically separated from four nonbonding bands, with the antibonding bands at higher energies. As the average valence of Mn is 3.5, there are two electrons in the e_g orbitals of the four Mn atoms that compose the chain. Hence the two bonding bands which have dominantly $d_{3x^2-r^2}$ character on atom 1 and $d_{3y^2-r^2}$ character on atom 3 are occupied. Thus, the one-dimensional chains which are a consequence of the magnetic structure drive the OO within these calculations. However, the difficulty in approaching the problem this way is that the $Immm$ structure exists only above the CO/OO temperature and there is extensive evidence in the literature suggesting a

symmetry lowering below the ordering transition. However, the details of the crystal structure of this compound are shrouded in controversy. It was suggested [6] that the structure, within the charge ordered state, is $Cmmm$ with lattice constants equal to $\sqrt{2}\,a$, $\sqrt{2}\,a, c$ where a and c are the cell dimensions of the basic $Immm$ cell. More recent work by Larochelle [15] however, indicates that the structure is $Ammm$ or one of its two subgroups $Am2m$ or $A222$, with the lattice parameters being $\sqrt{2}\,a$, $2\sqrt{2}\,a$, and c. None of the structural investigations have been able to provide the atom positions, particularly for the oxygen sites, owing to the large unit cell and the existing data quality [15]. This work however suggests certain possible distortions of the oxygens, though not in agreement with Ref. [6]. In view of such uncertainties, we have optimized the structure of this system using $ab\ initio$ band structure calculations. The structure that we find (see Fig. 1) is $Bbmm$ with lattice parameters $\sqrt{2}\,a$, $2\sqrt{2}\,a$, and c. The lattice parameters are in agreement with what was observed in [15].

On optimizing the internal coordinates, the system exhibited different distortions of the MnO_6 octahedra associated with different Mn atoms. The direction of displacement of the oxygen atoms in the ab plane is indicated by the arrows shown in Fig. 1b, though the oxygen atoms have been left out of the figure for added clarity. The Mn site, Mn(3), showing $d_{3y^2-r^2}$ OO lowered its energy by an elongation of the Mn-O bonds in the y direction. This kind of distortion can be understood easily within the framework of crystal-field effects. A tetragonal distortion of a MnO_6 octahedron resulting in an elongation of the Mn-O bond lengths in the y direction lowers the bare energy of the $d_{3y^2-r^2}$ orbital. Thus, the sites Mn(1) and Mn(3) behave as Mn^{3+} species, sustaining a Jahn-Teller (JT)-like distortion of the surrounding oxygens in two mutually perpendicular directions, giving rise to the orbital ordering. As a consequence, the oxygen atoms surrounding the sites labeled Mn(2) and Mn(4) sustain distortions with the oxygen atoms along the x axis being displaced in one direction and the ones along the y axis being displaced in another direction, as shown in the figure, in contrast to the suggestion in Ref. [6] where all four oxygen atoms surrounding the Mn^{4+} site move closer to the Mn atom. We found the kind of distortion suggested in that work to have a higher energy. The sites Mn(2) and Mn(4) have been identified as Mn^{4+} sites in the literature and we retain that nomenclature, although within our calculations the charge difference between the so-called Mn^{3+} and Mn^{4+} species is negligible.

While our calculations suggest different distortions of the surrounding oxygens about the Mn^{3+} and Mn^{4+} sites, the actual magnitude of the distortion is fairly small [16]. The underestimation of the magnitude of the JT distortion by these first principles approaches is well known, though these methods do get the nature of distortions correctly. An example of this is $LaMnO_3$ where the nature of distortion was correctly predicted, while the magnitude of the

theoretical JT distortion was found to be half of the experimental value [11]. We simulated the neutron diffraction pattern using the optimized coordinates as well as the coordinates [17] assuming a Jahn-Teller distortion equal to what is found in $LaMnO_3$. The simulated diffraction patterns were nearly identical, indicating the difficulty of determining the oxygen positions with any precision from such measurements. Therefore the enhanced distortion of the oxygen octahedra is not inconsistent with the structural data available so far. We in fact hope that the present theoretical considerations will help in the future structural investigations. It is also significant that with optimized JT distortion, the correct ground state magnetic order cannot be reproduced for $LaMnO_3$ [11]. The situation seems to be the same in the present case, where the CE-type antiferromagnetic state is more stable than the ferromagnetic state only with the enhanced JT distortion, consistent with earlier observations [18]. Hence in the subsequent analysis, we have extrapolated the magnitude of the JT distortion to the value observed in $LaMnO_3$.

The experiments of Murakami *et al.* [4] analyzed the energy dependence of the OO superlattice reflection across the Mn K absorption edge. The strong energy dependence was interpreted as arising from a splitting of ~5 eV between the $4p_x$ and $4p_y$ partial densities of states (DOS) at the sites Mn(1) and Mn(3) which show OO. While the $4p_x$ states were suggested to be 5 eV lower than the $4p_y$ on one Mn atom, the order was reversed on the other Mn atom. Theoretically there are two contrasting interpretations possible for such a splitting. Ishihara and Maekawa [19] argued in the context $LaMnO_3$ that the splitting in the Mn $4p$ states induced by the intra-atomic p-d Coulomb interaction produces such a strong tensor character of the scattering form factor. However, it was pointed out [20] that as the $4p$ states are extended, the suggested p-d Coulomb interaction strength is unphysically large and the splitting in the $4p$ states is actually caused by the JT distortion, though Coulomb interactions, particularly within the Mn $3d$ manifold, may have important consequences for other properties in such systems. These suggestions are consistent with an earlier analysis of transition metal K-edge x-ray absorption in Fe and Co oxides [21].

In Fig. 2 we plot the Mn $4p_x$ and $4p_y$ partial DOS in the energy range 10–20 eV above the Fermi level, projected onto the Mn site [Mn(1)] showing $d_{3x^2-r^2}$ ordering. A splitting of ~3 eV is clearly visible, with the $4p_x$ states located at lower energies. The order is reversed at the other Mn site [Mn(3)] which shows $d_{3y^2-r^2}$ ordering. Thus, our results on $La_{0.5}Sr_{1.5}MnO_4$ are consistent with the suggestion [20] in the context of $LaMnO_3$ that the JT distortion to be not only the driving force for the orbital ordering, but also responsible for the specific experimental effect of the pronounced tensor character of the form factor via the splitting of the $4p$ partial DOS.

Strong enhancement in the intensity at the energy corresponding to the absorption edge of Mn^{3+} was observed at the CO superlattice reflection [4]. These results sug-
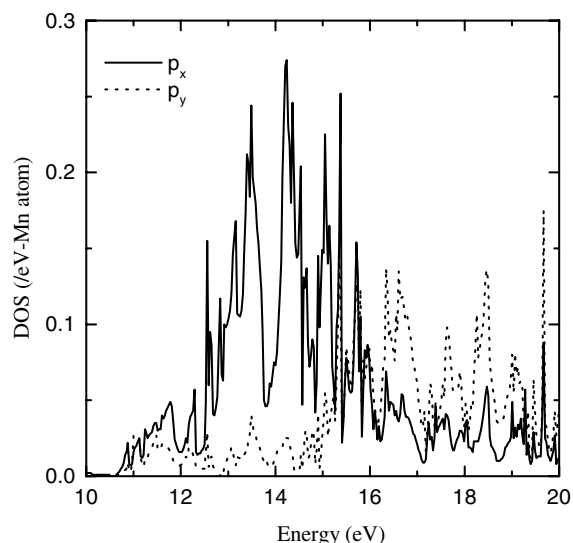

FIG. 2.　The Mn $4p_x$ (solid line) and $4p_y$ (dotted line) partial DOS projected onto the Mn^{3+} site showing $d_{3x^2-r^2}$ ordering.

gested the presence of a second Mn atom in the system, with its absorption edge 4 eV higher than that for the Mn^{3+} atoms. As the absorption edge for Mn^{4+} atoms lies ~4 eV above the absorption edge for Mn^{3+} atoms, they claimed that this was a direct evidence of an ordering of the two charge species—Mn^{3+} and Mn^{4+} in this system. From the present calculations, we find that as the environment for the Mn^{3+}-like sites is different from the environment for the Mn^{4+}-like sites, there is a substantial modification in the Mn $4p$ partial DOS, though the net charges associated with these two sites, 4.53 at Mn 1 and 3, and 4.51 at Mn 2 and 4, are almost identical. Hence, the modifications at the so-called CO superlattice reflection cannot be interpreted on the basis of a substantial difference in the charge state of the two inequivalent sites. Interestingly, our results for the electronic structure at these two sites provide a natural explanation for the observed results. With the x and y axes defined in Fig. 1 we have the $4p_x$ states at $Mn^{3+}(1)$ at lower energies compared to the Mn $4p_x$ states at Mn^{4+} site (Fig. 3). As a result we have an intensity maximum at the CO superlattice reflection. If the axes are rotated by 45°, one finds that the Mn $4p_{x'}$ states at $Mn^{3+}(1)$ and those at the Mn^{4+} site almost coincide (inset in Fig. 3). This results in a minimum in the intensity. A similar angular dependence is also observed at the OO superlattice reflection. Our reinterpretation is supported by recent experiments on $Nd_{0.5}Sr_{0.5}MnO_3$ [22] which also found a similar angular dependence of the intensity at a CO superlattice reflection.

In conclusion, we have carried out an analysis of the experimental observation for orbital and charge orderings in $La_{0.5}Sr_{1.5}MnO_4$. Our results indicate the presence of two Mn species with very different environments. One of the Mn species has a JT distortion of the oxygens surrounding that atom and hence, in this sense, behaves as an Mn^{3+} species. The distortions around the so-called Mn^{4+} atoms are different from the simple breathing mode distortion suggested earlier. Extrapolating the magnitude of the JT
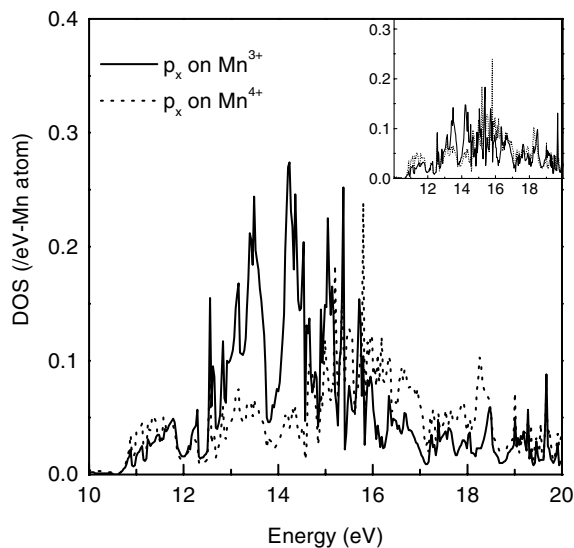
FIG. 3.   The $4p_x$ partial DOS at the Mn^{3+} (solid line) and Mn^{4+} sites (dotted line) are shown for the x and y axes defined in Fig. 1, and in the inset for x' and y' axes defined in Fig. 1.

distortion around the Mn^{3+} to equal the value observed in $LaMnO_3$ is necessary to obtain the correct description of the magnetic ground state. Further, the energy dependence at the orbital ordering as well as the charge ordering superlattice reflections can be explained by the distortions of the MnO_6 octahedra. The present results establish that no substantial real space charge ordering needs to be invoked in this system in order to explain the experimentally observed results; instead band structure effects are responsible for the dependence of the superlattice intensities on the energy and the orientation. The above interpretation is consistent with the observation that both charge ordering as well as the orbital ordering show the same temperature dependence. As the origin of the intensity variation observed at both reflections is the same, namely, the lattice distortions, our results explain why the charge ordering as well as the orbital ordering transition occurs over the same temperature range in this system.

Note added.— After the acceptance of our manuscript we came across a recent paper [23] on 50% doped three-dimensional manganites which have arrived at similar conclusions concerning the absence of any substantial charge ordering.

*Presently at NREL, Golden, CO.
†Also at Jawaharlal Nehru Center for Advanced Scientific Research, Bangalore, India.

 [1] Jeroen van den Brink, Giniyat Khaliullin, and Daniel Khomskii, Phys. Rev. Lett. **83**, 5118 (1999); Branko P. Stojkovic *et al.,* Phys. Rev. Lett. **82**, 4679 (1999); R. Mahendiran *et al.,* Phys. Rev. Lett. **82**, 2191 (1999); Wei Bao *et al.,* Phys. Rev. Lett. **78**, 543 (1997).
 [2] R. Osborn *et al.,* Phys. Rev. Lett. **81**, 3964 (1998); J. Q. Li *et al.,* Phys. Rev. Lett. **79**, 297 (1997).
 [3] Y. Murakami *et al.,* Phys. Rev. Lett. **81**, 582 (1998).
 [4] Y. Murakami *et al.,* Phys. Rev. Lett. **80**, 1932 (1998).
 [5] J. C. Bouloux *et al.,* Mater. Res. Bull. **16**, 855 (1981).
 [6] B. J. Sternlieb *et al.,* Phys. Rev. Lett. **76**, 2169 (1996).
 [7] J. H. Jung *et al.,* Phys. Rev. B **61**, 6902 (2000).
 [8] M. v. Zimmermann *et al.,* Phys. Rev. Lett. **83**, 4872 (1999).
 [9] Y. Wakabayashi *et al.,* J. Phys. Soc. Jpn. **69**, 2731 (2000).
[10] H. Nakao *et al.,* Phys. Rev. Lett. **85**, 4349 (2000).
[11] H. Sawada *et al.,* Phys. Rev. B **56**, 12 154 (1997).
[12] J. P. Perdew, K. Burke, and M. Ernzerhof, Phys. Rev. Lett. **77**, 3865 (1996).
[13] J. Lee, J. Yu, and K. Terakura, J. Korean Phys. Soc. **33**, S55 (1998).
[14] I. V. Solovyev and K. Terakura, Phys. Rev. Lett. **83**, 2825 (1999).
[15] S. Larochelle *et al.,* cond-mat/0101294.
[16] In the present structural optimization, the longer Mn-O distance and the shorter one at sites 1 and 3 are 1.98 and 1.90 Å, respectively. Similarly at sites 2 and 4, they are 1.89 and 1.96 Å.
[17] The longer Mn-O distance and the shorter one in the *ab* plane are 2.06 and 1.81 Å, respectively for both Mn^{3+} and Mn^{4+} sites.
[18] T. Mizokawa and A. Fujimori, Phys. Rev. B **56**, R493 (1997).
[19] S. Ishihara and S. Maekawa, Phys. Rev. Lett. **80**, 3799 (1998); Phys. Rev. B **58**, 13 442 (1998).
[20] I. S. Elfimov, V. I. Anisimov, and G. A. Sawatzky, Phys. Rev. Lett. **82**, 4264 (1999); Maurizio Benfatto, Yves Joly, and Calogero R. Natoli, Phys. Rev. Lett. **83**, 636 (1999); M. Takahashi, J. Igarashi, and P. Fulde, J. Phys. Soc. Jpn. **68**, 2530 (1999).
[21] Z. Y. Wu *et al.,* Phys. Rev. B **56**, 2228 (1997).
[22] K. Nakamura *et al.,* Phys. Rev. B **60**, 2425 (1999).
[23] J. Garcia, M. C. Sanchez, G. Subias, and J. Blasco, J. Phys. Condens. Matter **13**, 3229 (2001); J. Garcia *et al., ibid.* **13**, 3243 (2001).